schätzung der Korrelationsreichweite möglich. Voraussetzung für eine Glättung nach dem beschriebenen Verfahren ist immer, dass der Abstand zwischen den Messpunkten kleiner ist, als der durch die Korrelationsreichweite L gegebene maximale Samplingpunktabstand $\Delta b = 1/2\, L$. Dies ist jedoch bei praktischen Messungen erfahrungsgemäss immer der Fall. Oelschlaeger (1969) hat ein der beschriebenen Glättung verwandtes Verfahren ausgearbeitet, aus fehlerbehafteten Messwerten an beliebigen Stützpunkten genauere Werte der Streufunktion an den Sampling-Punkten zu gewinnen. Ein unserer Meinung nach wichtiger Vorteil der beschriebenen Methode besteht darin, Längen- und Breitenentschmierung in einem Rechengang durchführen zu können.

Die Glättung passt sich dabei organisch in die Rechnung ein. Verfahren, die ohne Glättung arbeiten, können grundsätzlich nur die fehlerbehaftete Streukurve entschmieren. Die Berücksichtigung einer Abschätzung der Korrelationsreichweite nutzt nur bekannte physikalische Tatbestände zur Glättung aus. Eine weitergehende Glättung wäre nur möglich, wenn der mathematische Typ der Streufunktion von vorneherein bekannt wäre. Um ihn zu ermitteln und damit Strukturuntersuchungen durchzuführen, werden aber gerade die Streuexperimente durchgeführt.

Für Diskussionen und die Überlassung von Manuskripten sowie weiterer Unterlagen möchten wir den Herren Prof. Dr O. Kratky, Dr H. Oelschlaeger, Dr H. Leopold aus Graz, Herrn N. Smirnov aus Puschtschino und Herrn Dr F. Hossfeld aus Jülich unseren verbindlichen Dank aussprechen.

Literatur

DAMASCHUN, G., KLEY, G., MÜLLER, J. J. & PÜRSCHEL, H.-V. (1968). *Acta biol. med. germ.* **20**, 409.

DAMASCHUN, G., MÜLLER, J. J. & PÜRSCHEL, H.-V. (1968*a*). *Mh. Chem.* **99**, 2343.

DAMASCHUN, G., MÜLLER, J. J. & PÜRSCHEL, H.-V. (1968*b*). *Acta biol. med. germ.* **20**, 379.

DAMASCHUN, G. & PÜRSCHEL, H.-V. (1969). *Mh. Chem.* **100**, 274.

DAMASCHUN, G. & PÜRSCHEL, H.-V. (1971). *Acta Cryst.* Im Druck.

DEBYE, P. (1915). *Ann. Phys. Lpz.*, **46**, 809.

DEBYE, P. (1927). *Phys. Z.* **28**, 135.

DIJKSTRA, A., KORTLEVE, G. & VONK, C. G. (1966). *Kolloid-Z. und Z. Polymere*, **210**, 121.

FJEDOROV, B. A. (1968). *Kristallografiya*, **13**, 763.

FJEDOROV, B. A., ANDREJEVA, N. A., VOLKOVA, L. A. & VORONIN, L. A. (1968). *Kristallografiya*, **13**, 770.

HEINE, S. & ROPPERT, J. (1962). *Acta Phys. Austr.* **15**, 148.

HOSEMANN, R. & BAGCHI, S. N. (1962). *Direct Analysis of Diffraction by Matter.* Amsterdam: North-Holland Publishing Co.

HOSSFELD, F. (1968). *Acta Cryst.* A**24**, 643.

HOSSFELD, F. & MAIER, G. (1967). *Z. angew. Phys.* **22**, 145.

KRATKY, O., POROD, G. & SKALA, Z. (1960). *Acta Phys. Austr.* **13**, 76.

KRATKY, O. (1967). In *Proc. Conf. held at Syracuse Univ.* 1965, *Small-Angle X-ray Scattering.* H. BRUMBERGER (Hrsg.). New York, London, Paris: Gordon & Breach.

LAKE, J. A. (1967). *Acta Cryst.* **23**, 191.

LAKE, J. A. & BEEMANN, W. W. (1968). *J. Mol. Biol.* **31**, 115.

MACKE, W. (1961). *Wellen.* Leipzig: Geest & Portig K.-G.

MAZUR, J. & WIMS, A. M. (1966). *J. Res. Nat. Bur. Stand.* **70**A, 467.

OELSCHLAEGER, H. (1969). Private Mitteilung.

POROD, G. (1951). *Kolloid-Z. und Z. Polymere*, **124**, 83.

POROD, G. (1951). *Kolloid-Z. und Z. Polymere*, **125**, 51.

RALSTON, A. & WILF, H. S. (1960). In *Mathematical Methods for Digital Computers.* New York, London: John Wiley.

SCHMIDT, P. W. (1955). *Acta Cryst.* **8**, 772.

STOKES, A. R. (1948). *Proc. Phys. Soc. London*, **61**, 38.

TAYLOR, T. R. & SCHMIDT, P. W. (1967). *Acta Phys. Austr.* **25**, 293.

Acta Cryst. (1971). A**27**, 18

The Energy Flow of X-rays in Silicon Single Crystals

BY L. GERWARD

Department of Physics, Chalmers University of Technology, Fack, S-402 20 Göteborg 5, Sweden

(*Received* 22 *September* 1969 *and in revised form* 14 *January* 1970)

The angular divergence of the energy flow of anomalously transmitted X-rays in nearly perfect silicon crystals has been determined experimentally from image widths of dislocations on X-ray topographs. Anomalous transmission of copper, iron, and chromium radiation has been used. The result is compared with calculations using the dynamical theory of diffraction. It is shown that the angular divergence is almost constant regardless of the X-ray wavelength and that it can be made to decrease only by increasing the crystal thickness.

Introduction

According to the dynamical theory of diffraction a number of wave fields are produced in a crystal when an incident wave satisfies the Bragg condition for a particular set of lattice planes. The situation is described with the aid of the dispersion surface in reciprocal space. Each wave field corresponds to a point on

this surface (tiepoint) and produces an energy flow in the direction of the normal to the surface (von Laue, 1960; Kato, 1958).

In the Laue case for a thick crystal, *i.e.* $\mu t \gg 1$, where μ is the normal photoelectric absorption coefficient and t is the crystal thickness in the direction of the incident beam, only wave fields belonging to one branch of the dispersion surface will reach the exit surface of the crystal owing to reduced absorption. This phenomenon is known as anomalous transmission or the Borrmann effect.

Crystal defects such as dislocations will destroy the anomalous transmission and may be recorded as 'shadows' on a photographic plate. The effect has been widely used for the study of dislocations in nearly perfect crystals, for instance by Borrmann, Hartwig & Irmler (1958), Meier (1962), and Young, Baldwin, Merlini & Sherrill (1965). Recent reviews on the contrast in dislocation images have been given by Bonse (1964) and Authier (1966).

Owing to selective absorption, the direction of the energy flow is confined to a certain angular range around a direction parallel to the diffracting lattice planes. Young *et al.* (1965) observed the width of dislocation images in order to determine the effective angular divergence of the energy flow. However, they had no accurate method for measuring the distance from the dislocation to the exit surface.

In this work dislocations running from the front to the back surface of the specimen have been used for the study of image widths. The angle of inclination of the dislocation line with respect to the surface is determined on topographs recorded by hard radiation ($\mu t < 1$) and in this way the distance from each point on the dislocation line to the exit surface is determined. The angular divergence of the energy flow has been studied for several X-ray wavelengths in order to cover a wide range of the value of μt.

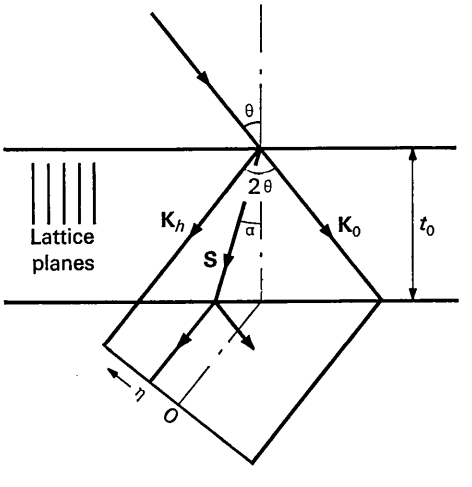

Fig. 1. Ray diagram of symmetric Laue case. $\mathbf{K}_0$ = wave-vector of direct beam; $\mathbf{K}_h$ = wave-vector of diffracted beam; S = Poynting vector; t_0 = crystal thickness.

Theory

Intensity distribution in the diffracted beam

Consider the symmetrical Laue case shown in Fig. 1. The theory is also simplified by considering a centrosymmetrical structure with origin of coordinates at a symmetry centre, which case applies to silicon. The notation used here is in the main the same as that of von Laue (1960).

Starting from $\Delta\theta$, the departure of the incident beam direction from the Bragg angle θ, it is convenient to define two variables y and v_r

$$y = \sinh v_r = \frac{\Delta\theta \sin 2\theta}{C|\chi_{rh}|}, \qquad (1)$$

where C is the polarization factor which equals unity or $|\cos 2\theta|$ for the σ polarization state and for the π state, respectively, and $\chi_h = \chi_{rh} + i\chi_{ih}$ is the Fourier coefficient of the dielectric susceptibility.

The energy flow of the wave field inside the crystal is described by the Poynting vector S which will make an angle α with the lattice planes. For a wave field belonging to the dispersion surface of reduced absorption the absorption coefficient with respect to the direction of S is given by

$$\mu_S = \mu \frac{\cos\alpha}{\cos\theta}[1 - C\varepsilon(1-p^2)^{1/2}], \qquad (2)$$

where

$$\varepsilon = (\chi_{ih}/\chi_{i0}) \exp(-M),$$
$$p = \mathrm{tg}\alpha/\mathrm{tg}\,\theta, \quad -1 \le p \le 1.$$

Thermal motion is included through the Debye–Waller factor M.

For a 220 reflexion in silicon ε very nearly equals unity and the main departure from unity is given by the Debye–Waller factor.

It can be shown that the direction of the energy flow is related to the departure from the Bragg condition by

$$p = \mathrm{tgh}\, v_r. \qquad (3)$$

At the exit surface the energy flow of the wave field decomposes into a diffracted beam and a direct beam. The reflecting power, *i.e.* the ratio of the diffracted energy to the incident energy is given by

$$R = \frac{1}{4\cosh^2 v_r} \exp(-\mu_S t_S), \qquad (4)$$

where

$$t_S = t_0/\cos\alpha.$$

Under the experimental conditions used in this work the angular divergence of the incident beam is large enough to cover the whole range of reflexion which is only about ten seconds of arc. Thus wave fields with all directions within the energy-flow triangle contained between the direct and diffracted beam

directions are produced. Kato (1960) has derived a general expression for the intensity distribution at the exit surface due to a polarized incident beam taking both branches of the dispersion surface into account. Here only the branch of least absorption contributes but both states of polarization have to be considered.

Suppose that the incident beam is unpolarized and that its intensity is constant within the range of reflexion,

$$I_0^{(a)}(\Delta\theta)=\text{const.} \tag{5}$$

The incident power in the angular range corresponding to dy may be expressed as

$$\mathrm{d}P_0^{(a)}=I_0(1+C)\,\mathrm{d}y\,, \tag{6}$$

where I_0 is a constant factor and $C=|\cos 2\theta|$. The first and second terms in the parenthesis of equation (6) represent the contributions of the σ and π polarization components, respectively. Let the index i describe the state of polarization. Following Kato (1960) the intensity distribution of the diffracted beam along the η axis of Fig. 1 is expressed as

$$I_{h,i}(\eta)=R_i\frac{\mathrm{d}P_{0,i}^{(a)}}{\mathrm{d}\eta}=R_i\frac{\mathrm{d}P_{0,i}^{(a)}}{\mathrm{d}y}\cdot\frac{\mathrm{d}y}{\mathrm{d}v_r}\cdot\frac{\mathrm{d}v_r}{\mathrm{d}p}\cdot\frac{\mathrm{d}p}{\mathrm{d}\eta}$$
$$i=\sigma,\pi\,. \tag{7}$$

Inserting equations (1) to (6) in equation (7) and adding the contributions of the two polarization components gives the total diffracted intensity.

$$I_h(\eta)=\frac{I_0}{4t_0\sin\theta}\,\frac{\exp(-\mu t)}{(1-p^2)^{1/2}}\left\{\exp[\mu t\varepsilon(1-p^2)^{1/2}]+C\exp[C\,\mu t\varepsilon\,(1-p^2)^{1/2}]\right\}, \tag{8}$$

where

$$t=t_0/\cos\theta\,.$$

Intensity distribution on a traverse topograph

When the crystal is traversed or a long focus line is used each point on the exit surface receives an intensity which is integrated over all values of p. However, if the crystal contains a disturbed volume *e.g.* surrounding a dislocation, the disturbance will destroy the anomalous transmission in the directions of the incident wave fields. This phenomenon may be described by saying that the disturbed volume will cast a shadow on to the exit surface of the crystal. The angular divergence of this shadow is described by equation (8).

Consider a dislocation lying in the diffracting lattice planes as shown in Fig. 2. Suppose that the effective angular divergence of the shadow is given by $\Delta\alpha$. At the exit surface the shadow will have a width W given by

$$W=2[R+z\,\mathrm{tg}(\Delta\alpha/2)]\,, \tag{9}$$

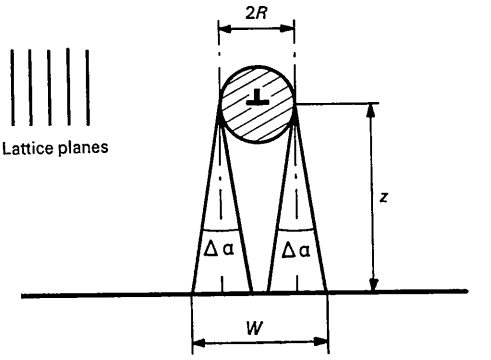

Fig. 2. Dislocation image due to angular divergence of the energy flow.

where R = radius of the disturbed volume,
z = distance from the exit surface.

Thus by determining the width as a function of z it should be possible to determine $\Delta\alpha$ experimentally. For comparison with the theory $\Delta\alpha$ is evaluated from the half maximum value according to equation (8).

Experimental procedure

The silicon crystals used for these studies are rectangular wafers $15\times20\times0{\cdot}39$ mm in size, containing only a few dislocations per cm^2. The large lateral surface is a (110) plane and the edges are along the [$\bar{1}$10] and [001] directions.

Topographs of the crystals were made using Lang's (1959) traverse technique.

Dislocation images were recorded by anomalous transmission of copper, iron, and chromium $K\alpha$ radiation. The values of μt are 6·2, 12·7, and 22·1, respectively. The $\bar{2}20$ reflexion was used throughout.

The lengths of the dislocation lines were determined on topographs recorded by silver and molybdenum $K\alpha$ radiation, ($\mu t=0{\cdot}32$, and 0·64, respectively). The measurements were made on the original topographs using a travelling microscope.

On topographs reproduced here an arrow indicates the projection of the diffraction vector on to the image plane.

Results

Dislocations running from the front to the back surface of the crystal give rise to a delta-shaped image on anomalous transmission topographs due to the angular divergence of the energy flow. The sharp end of the image corresponds to the part near the exit surface.

Dislocations lying in the ($\bar{2}20$) plane used for diffraction were chosen and the angles of the delta-shaped images were determined on the topographs. Some images of this kind are shown in Fig. 3.

Fig. 4 shows the same dislocations on a topograph recorded by molybdenum $K\alpha$ radiation. Here $\mu t<1$

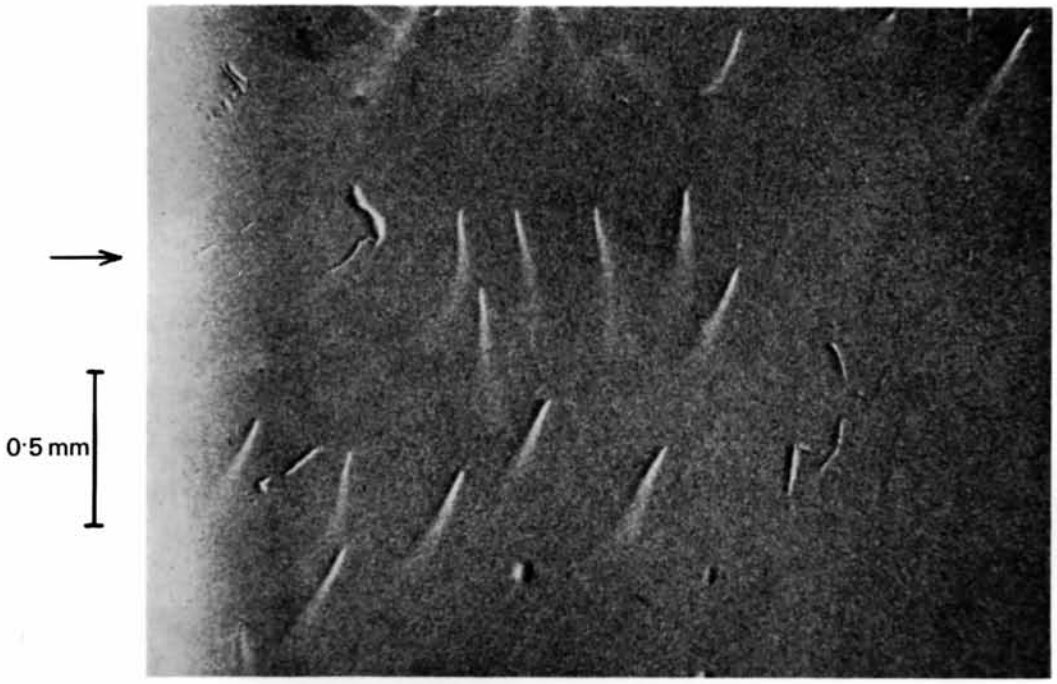

Fig. 3. Traverse topograph of silicon. $\bar{2}20$ reflexion, Fe $K\alpha_1$.

Fig. 4. Traverse topograph of silicon. $\bar{1}11$ reflexion, Mo $K\alpha_1$.

[To face p. 20

which means that the image contrast is reversed and the full length of each dislocation line is seen.

The angle of inclination of the dislocation with respect to the surface is determined from the length of the dislocation line on the topograph and the thickness of the crystal. Thus the distance from each point of the dislocation line to the exit surface is determined and the angular divergence of the energy flow follows from equation (9).

Fig. 5 shows plots of intensity profiles according to equation (8) using the experimental values of $\mu t\varepsilon$. From data of the Debye–Waller factor given in *International Tables for X-ray Crystallography* (1962) it is estimated that $\varepsilon=0{\cdot}97$ for a 220 reflexion in silicon. The widths at half maximum have been determined from the plots.

Table 1 summarizes the experimental and theoretical results.

Table 1. *Angular divergence of the energy flow of X-rays in silicon*

$t_0=0{\cdot}39$ mm, $\varepsilon=0{\cdot}97$.

		Experimental		Theoretical	
λ	$\mu t\varepsilon$	$\Delta p/2$	$\Delta\alpha$	$\Delta p/2$	$\Delta\alpha$
1·54 Å	6·0	0·36	18°	0·51	25·2°
1·94	12·3	0·29	18	0·35	23·2
2·29	21·4	0·19	16	0·26	21·8

The experimental error in the values of $\Delta\alpha$ is estimated to be $\pm 1°$.

Discussion

The experimental values of the angular divergence of the energy flow are found to be smaller than the theoretical ones as shown in Table 1. A probable reason is that the theoretical model used here is oversimplified.

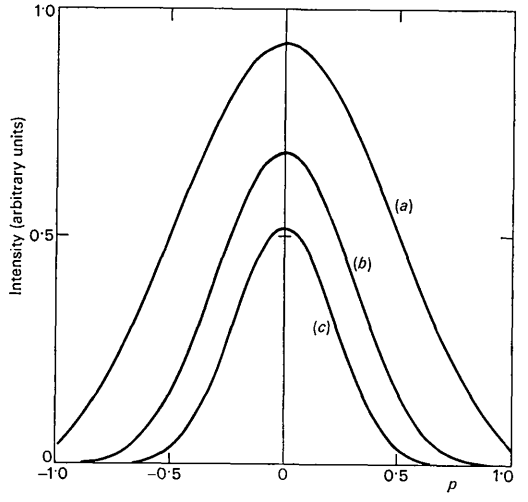

Fig. 5. Intensity profile of the diffracted beam, (*a*) $\mu t\varepsilon=6{\cdot}0$; (*b*) $\mu t\varepsilon=12{\cdot}3$; (*c*) $\mu t\varepsilon=21{\cdot}4$.

Actually the situation is more complicated, as discussed in the reviews by Bonse (1964) and Authier (1966). The dislocation is not a discontinuous lattice defect but consists of a strain field continuously decreasing as $1/r$, where r is the distance from the dislocation line.

Wave fields incident on the highly distorted region near the dislocation core will create new wave fields (interbranch scattering) which will be absorbed. The result is a decrease of intensity in the directions of the incident wave fields *i.e.* the dislocation will cast a shadow.

However, wave fields incident on the lightly distorted regions away from the dislocation line may adapt themselves to the slowly varying state of the lattice and follow curved paths. Paths resulting from this process have been calculated by Kambe (1963) for wave fields incident on an edge dislocation in germanium.

In Table 1 it is also seen that the angular divergence is nearly constant in the region around 20° for all values of μt. This seems surprising at first sight since it is often stated in the literature that for large values of μt the energy flow should be practically parallel to the lattice planes. The reason for this discrepancy is the way in which a large value of μt has been achieved, as will be shown below.

Neglecting the contribution from the π state of polarization an approximate expression for the width Δp at half maximum according to equation (8) is given by

$$\Delta p/2 \simeq \left(\frac{2\ln 2}{\mu t\varepsilon - 1}\right)^{1/2} . \qquad (10)$$

Thus for large values of μt, $\Delta p \propto (\mu t)^{-1/2}$. Now $\mu \propto \lambda^3$ provided that no absorption edge is included in the wavelength range, $\lambda \propto \sin\theta$, and $t=t_0/\cos\theta$. It follows that

$$\mathrm{tg}(\Delta\alpha/2) \propto \mathrm{tg}^{1/2}\theta/\sin\theta . \qquad (11)$$

For $\theta<\pi/4$ this function decreases with increasing θ but within the θ range used here the variations are small.

Thus a large value of μt does not always mean a highly collimated energy flow. If μ is increased by using more absorbant radiation the increased value of μt is compensated by a correspondingly larger Bragg angle in the energy flow triangle. The only way to reduce the angular divergence of the energy flow to an appreciable extent is to use thicker crystals. For instance $\Delta\alpha=4°$ would require a silicon crystal about 1·5 cm thick, according to equation (10).

The author wishes to thank Professor G. Brogren for his kind interest during the course of this work and for many stimulating discussions. A grant from Statens Naturvetenskapliga Forskningsråd is gratefully acknowledged.

References

AUTHIER, A. (1966). *Advanc. X-ray Anal.* **10**, 9.
BONSE, U. (1964). *Z. Physik*, **177**, 543.
BORRMANN, G., HARTWIG, W. & IRMLER, H. (1958). *Z. Naturforschg.* **13a**, 423.
International Tables for X-ray Crystallography (1962). Vol. III, p. 237. Birmingham:Kynoch Press.
KAMBE, K. (1963). *Z. Naturforsch.* **18a**, 1010.
KATO, N. (1958). *Acta Cryst*, **11**, 885.
KATO, N. (1960). *Acta Cryst.* **13**, 349.
LANG, A. R. (1959). *Acta Cryst.* **12**, 249.
LAUE. M. VON (1960). *Röntgenstrahlinterferenzen.* Frankfurt am Main: Akademische Verlagsgesellschaft.
MEIER, F. (1962). *Z. Physik*, **168**, 10.
YONG, F. W., BALDWIN, T. O., MERLINI, A. E. & SHERRILL, F. A. (1965). *Advanc. X-ray Anal.* **9**, 1.

Acta Cryst. (1971). A**27**, 22

Diffraction Intensities from a Cluster of Curved Crystallites. III. The Three-Dimensional Case

BY G. B. MITRA AND S. BHATTACHERJEE

Department of Physics, Indian Institute of Technology, Kharagpur, India

(*Received* 24 *September* 1969)

A general expression for the intensity of X-rays diffracted by a conglomeration of identical cylindrical crystallites with a given angular opening and with axes oriented randomly with respect to the incident beam has been worked out. This expression leads directly to the expressions derived by Mitra for one- and two-dimensional curved crystallites. For cylindrical shells the peaks are highly asymmetrical. They become sharper and shift towards the higher-angle side as the shell axes become more tilted with respect to the normal to the plane containing the incident and the equatorially diffracted beams. The overall nature of the diffraction pattern remains the same. The effect of increasing the number of scattering centres on each arc is found to be only to increase the peak heights and their sharpnesses. The effect of radial thickness is to cause a peak shift and to give rise to additional peaks. The peak heights are increased and become sharper as the radial thickness increases. The effect of curvature is an increase in the number of peaks, an increase in the general background level of scattering and a decrease in the peak heights.

Introduction

In the course of two previous publications [Mitra (1965) and Mitra & Bhattacherjee (1968) hereafter referred to as I and II respectively], an elementary theory of diffraction by an axially parallel aggregate of curved crystallites has been developed and a general expression for two-dimensional curved crystals has been derived. In the treatment, both the incident and the diffracted beams have been assumed to lie in the same plane as the two-dimensional crystallites. The expression derived is satisfactory in the sense that for the extreme cases of zero curvature and of equiangularly spaced atoms arranged on the circumference of a circle, it leads, as expected, respectively to Bragg's law and to the expression derived by Blackman (1951) for a circular lattice. This expression has also the further property of taking into account the angular opening of the curved crystallites as is the case with the expression derived by Kunze (1956). A further virtue of this expression is that it is a finite series of terms containing Bessel functions of order zero (in contrast with infinite series of Bessel functions of very high order in the expression of the above authors) rendering the task of numerical evaluation comparatively easy. However, it would be more realistic to consider an agglomeration of identical cylindrical crystallites with a given angular opening and with axes oriented randomly with respect to the incident beam – in short, a powder of cylindrical fragments. In this paper, it has been attempted to achieve this.

Derivation of the general expression for diffraction intensity

Each crystallite is considered to be built up of an identical stacking of T identical layers of the type of $ABCD$ [Fig. 1(*a*)], the details being the same as in Fig. 1 of I. The stacking along the Z direction is at equal intervals, c, as shown in Fig. 1(*b*). The curvature lies in the XY plane. $ABCD$ consists of M concentric arcs at radial distances $R, R+b, R+2b, \ldots R+mb, \ldots R+(M-1)b$ respectively. Each arc has N lattice points arranged equiangularly on it so that two consecutive points on the same arc subtend an angle φ at the point of intersection of the axis OZ with the plane $ABCD$. The angular opening is denoted by a parameter Q where $Q=2\pi/N\varphi$. Any lattice point J [Fig.1(*b*)] in the cylindrical lattice occupies the rth site on the mth arc on the tth stack and is described by (r,m,t). The point A is